

# Evaluating Opportunities for Increasing Power Capacity of Existing Overhead Line Systems

**K. Kopsidas and S. M. Rowland**

The University of Manchester  
School of Electrical and Electronic Engineering,  
PO Box 88, Manchester, M60 1QD, UK.  
konstantinos.kopsidas@manchester.ac.uk

**Keywords:** AAAC, ACSR, ampacity, composite conductors, conductor creep, high temperature, overhead line, re-conductoring, re-tensioning, sag, wood pole structure.

## **Abstract**

Re-tensioning and/or re-conductoring are considered the most popular cost-effective ways to increase the efficiency of power capacity of an existing aerial line. The identification of the most beneficial method requires ampacity and sag calculations to consider all the system factors that influence its performance. A holistic methodology for calculating conductor ampacity and sag at any temperature and power frequency when different conductors are implemented onto a pre-specified overhead line structure is used to illustrate how the properties of the conductors allow opportunities for thermal and voltage uprating on existing Overhead Line Systems. This is achieved through a comparative analysis of the electrical and mechanical behaviour of conductors of different technologies and sizes on a 33 kV wood pole system. The analysis focuses on normal operating temperatures for novel conductors which can operate at elevated temperatures to avoid the increase in losses, and also allow the comparison with conventional conductors in order to identify potential benefits for the investigated OHL system.

## **1. Introduction**

The need to increase the power transfer capacity of existing overhead lines (OHL) by cost-effective and environmentally-friendly methods within a competitive deregulated market is directly linked with an increase in the associated conductors' ampacity (i.e. current capacity). Two of the most popular ways that can be employed to achieve this are re-tensioning and re-conductoring. The former is based on maximising the conductor's clearance to the ground by increasing its tension, allowing an increase in operating conductor thermal expansion facilitating higher current flows. Re-tensioning is usually applied in old lines for which the conductor sag is the limiting factor for increasing a line's thermal rating or on surveyed lines which experienced severe weather and electrical loading out of the predicted design conditions. Error in sag prediction may result in the need for line re-tensioning. This error is a common consequence of the misinterpretation of the conversion of conductor plastic elongation to thermal elongation, based on experimental data or standards [1].

Alternatively, re-conductoring involves replacing the existing conductors with conductors of larger sizes or alternative materials and technologies. Several new conductors have been designed and produced to yield an increase in power transfer capability. These technologies mainly attempt to increase the conductor's performance by increasing its maximum (continuous) operating temperature, therefore increasing its maximum current capacity. Moreover, recent composite designs like 'aluminium conductor composite reinforced' (ACCR) and 'aluminium conductor composite core' (ACCC) [2-3] are independent of steel's weight and coefficient of thermal expansion. This independence

may be the key to these conductors' improved performance at both normal as well as elevated operating temperatures. Such conductors are commonly called high temperature low sag (HTLS) conductors.

The implementation of changes required for upgrading an existing line are related to the cost, time and outages needed. The thermal upgrading of existing OHL by re-tensioning or re-conductoring is advantageous as it requires fewer modifications and less implementation time than other methods [4]. In contrast, voltage level upgrading involves more changes and takes more time to implement particularly when additional rights-of-way are required usually resulting in higher costs [5-6].

It should be emphasised that the existing literature [3-4, 7-9] evaluates the performance of different HTLS conductors by direct comparison with aluminium conductor steel reinforced (ACSR), as most HTLS conductors have a steel core as strength member, and not with the lighter and more conductive all aluminium alloy conductor (AAAC) type. Furthermore, limited work has been done to examine conductor performance with a realistic power line structure to evaluate the real benefits of HTLS conductors when compared with ACSR and AAACs. No evaluation of the improved performance conductors on aerial wood pole lines has been presented, apart from our recent analysis [10]. In that work we reported the improvement offered by re-conductoring in the power transfer capacity of a 33kV wood pole structure. The focus was mainly on the comparison of the mechanical and electrical performance of AAAC and ACSR conductors. To aid this comparison, a 'three sag zones' theory was proposed. In this

paper we build and extend this theory by identifying the critical properties of the conductors and their materials and the way these are affecting the zones. To do so we use a case study of a similar structure but different in respect to the limitations it poses to the system performance in order to extend the results, adding also more standard (American) conductor sizes. Furthermore, comparison of similar weight conductors is performed as this property is more critical for weak wood poles. In addition, analysis is performed for sag at different temperatures and different span lengths.

Hence, this paper focuses on conductors' properties that could allow opportunities for increasing the power capacity of an existing 33 kV wood pole OHL system. Such properties include the coefficient of thermal expansion, elasticity, strength and weight. In addition, analysis considers the effect of the increase in operating temperature on the ampacity, losses, and sag. This analysis is performed using the methodology described in the following section.

## **2. Methodology: A Holistic Perspective on Ampacity and Sag Computations**

The conductor's maximum current capacity limits the maximum power transfer capability of the OHL system. This current is usually referred to as ampacity and is limited by properties relevant to conductor design, the surrounding environment, operational conditions and the OHL structure design (as this defines the conductor size). These properties influence the elastic, plastic and thermal elongation which are proportional to conductor weight, tension, and current flow, respectively, and thus result in altering conductor sag. Sag defines the height difference between two points of the

conductor: one located at the suspension fittings and the other located at mid-span. Sag, therefore, defines the system's minimum ground clearance. There are two critical sag conditions considered during the design of an OHL system which define the maximum total (i.e. considering elastic, plastic and thermal) conductor elongation:

1. The maximum mechanical loading occurs at the designed maximum weather loading of the system (i.e. when ice is attached or wind is battering the conductor). This condition also yields the maximum conductor tension (MCT).
2. The maximum electrical loading, occurs when the tension is at the minimum because of the thermal elongation caused by the current flow. Usually, during these electrical loading conditions, the most severe sag and minimum ground clearance, limit any further increase in current flow. This current flow is affected by the ambient conditions, hence seasonal ampacities become common practice; these seasonal ampacities are defined by the average ambient conditions and maximum operating conductor temperature ( $T_{MAX}$ ).

The methodology which is briefly outlined here for the readers' convenience is detailed in [11-12]. The process is illustrated in the flowchart of Fig. 1 and emphasises the key electromechanical elements influencing conductor sag and ampacity calculations. The computations involved in this process are divided into three different steps which are performed separately and then linked together to compute the final conditions. Therefore, a holistic perspective on the system performance is taken by considering four different data groups for the calculations:

- Overhead line data of support structure (i.e. structure type and dimensions, tensile loading strength, weight strength, latitude, azimuth and elevation).

- Weather data (i.e. ambient temperature, wind speed, ice, pollution level).
- Conductor data (i.e. materials, number and shape of strands for the core and the outer strands, diameter of strand, grease pattern [13]).
- Operational data (i.e. frequency, maximum conductor temperature).

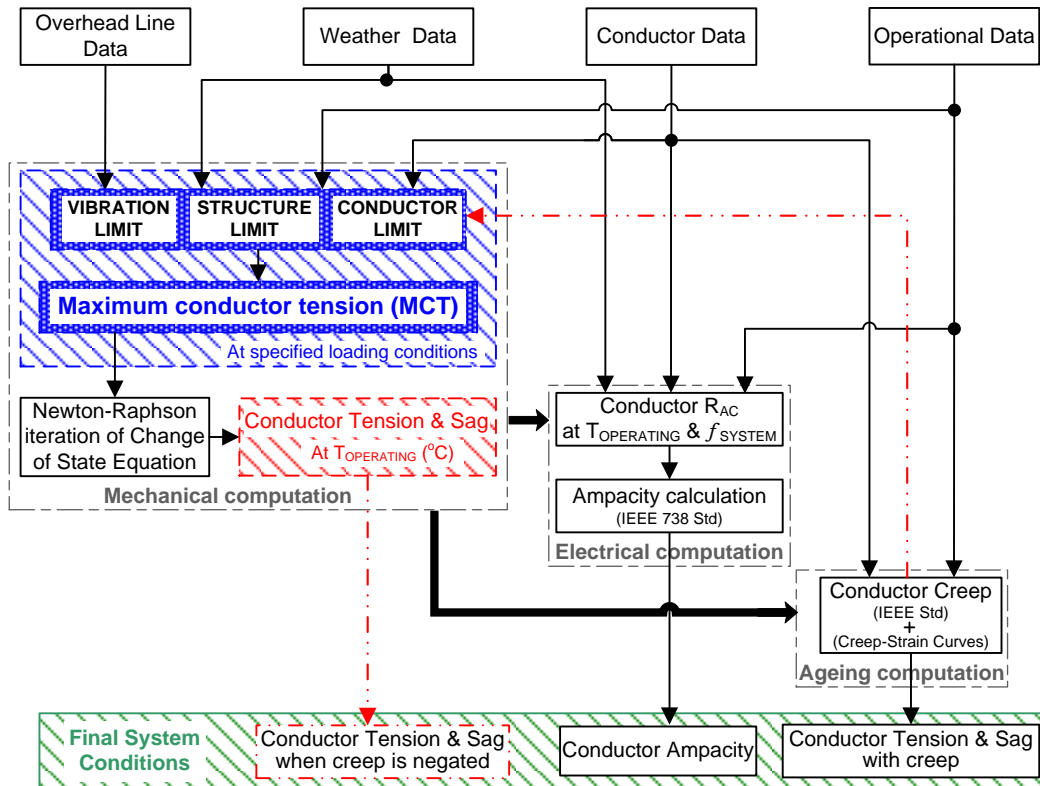


Figure 1

## 2.1. Mechanical Computations

This analysis determines the conductor sag and tension at the designed conductor  $T_{MAX}$ . In order to achieve this, the MCT of the conductor on a particular OHL system is required. This is controlled by the following limitations applicable to any structure and are highly dependent on the particular system: (a) structure limit (i.e. the maximum permitted tension allowed by the infrastructure strength and also influenced by the weather loading), (b) conductor limit (i.e. the maximum permitted conductor tension at

defined extremes of weather loading), and (c) vibration limit (i.e. the self-damping vibration limit tension of the conductor at everyday tension - EDT).

A Newton-Raphson iteration is then used on the change of state equation (1) (based on the catenary curve) to convert the vibration limit at EDT to the maximum weather loading conditions (e.g. including wind and ice at -5.6 °C):

$$f(F_{HF}) = \frac{2 \cdot F_{HF}}{W_F} \sinh\left(\frac{W_F \cdot \ell}{2 \cdot F_{HF}}\right) - \frac{2 \cdot F_{HI}}{W_I} \sinh\left(\frac{W_I \cdot \ell}{2 \cdot F_{HI}}\right) \cdot Th \cdot E\lambda = 0 \quad (1)$$

Where,  $F_{HI}$ ,  $F_{HF}$  are the initial and final horizontal tensions,(N).

$W_I$ ,  $W_F$  are the initial and final resultant conductor weights, (N/m).

$Th$  is the conductor thermal elongation, (m).

$E\lambda$  is the conductor elastic elongation, (m).

$\ell$  is the span length, (m).

This expression considers the elastic and thermal elongation while the irreversible plastic elongation (creep) is computed separately (Fig. 1). The three limitations are then compared at the maximum loading conditions and the smallest magnitude is set as the critical MCT of the examined system (see blue box in Fig. 1). Equation (1) is used again when the MCT of the system is known to compute the conductor tension and sag at the  $T_{MAX}$  set by the operator as illustrated in Fig. 1. This output (i.e. conductor tension and sag) is then linked with the other two computational steps (i.e. electrical and ageing). It should be noted that equation (1) does not consider the knee-point effect of some bi-material conductors and therefore its implementation results in larger sag values at elevated temperatures. Even though the knee-point is an important aspect of the operation of high temperature conductors (as these conductors take advantage of the decrease in the coefficient of thermal expansion above the knee-point), the conclusions derived from the

analysis in this paper are not affected by this limitation; in contrary the alteration of the methodology to address this limitation would result in slightly less sag than that reported here [2, 14].

It is also important to note that the conductor's greased weight and rated breaking strength (RBS) is calculated at this level from the physical design of the conductor and the material properties used [e.g. 13, 15-19]. Weather conditions are part of the OHL system and are considered in the computations as they affect safety factors and stresses. These safety factors are employed to provide a margin over the theoretical design capability to consider uncertainty in the design process as a requirement imposed by standards. Weather maps and/or historical data measurements can be used in order to identify the weather loading of the structure and the corresponding safety factors [13, 20-21].

## **2.2. Electrical Computations**

Electrical computations are performed to determine the AC resistance ( $R_{AC}$ ) of any conductor at any  $T_{MAX}$  defined from the mechanical computations. Basic electrical properties (e.g. resistivity, temperature coefficient of resistance) which are influenced by physical ones (e.g. spiralling factor, magnetisation effect, skin effect) are considered for the calculation of the conductor DC resistance ( $R_{DC}$ ) at  $T_{MAX}$ . The ASTM standards for the conductivity of different materials, temperature coefficients of resistance, and spiralling factors for cylindrical and trapezoidal strands are employed for the  $R_{DC}$  computation [13, 15-19].



The physical structure of the conductor is then used to compute its skin effect factor according to the methodology suggested by Dwight [22] and Lewis and Tuttle [23] and simplified further by using polynomials [24]. In the case of ACSR cable the magnetisation factor is also added to correct the  $R_{AC}$  as described elsewhere [25-26]. Once the  $R_{AC}$  computation step is completed the ampacity for the ambient conditions of the system is calculated using the IEEE standards [27].

The electrical computations described here, are developed to increase the flexibility and accuracy of the calculation of  $R_{AC}$ . Accuracy is improved by the direct calculation of the  $R_{AC}$  for any conductor rather than by using the linear interpolation of the tabulated values in [26] or manufacturers' data sheets as suggested in the standard's method [27]. To evaluate the methodology's accuracy for these calculations, a comparison was performed between the estimated  $R_{AC}$  for different conductors with the corresponding data provided by different manufacturers and yielded a negligible difference (<0.5%) [11-12].

### **2.3. Ageing Computations**

This section considers the conductor ageing which is the result of the long-term plastic elongation (creep-strain effect), the short-term influence of elevated conductor operating temperatures and the maximum tensile loads. Consideration is given to creep developed during a conductor's designed life time for the operating conditions and the conductor temperature defined in the mechanical computation part. The long term creep is defined by the system's every day operating conditions and is usually computed for 10 years. The elevated temperature occurs when aluminium conductors operate above 75 °C or steel-reinforced conductors operate above 100 °C [28-29]. The creep developed due to

maximum conductor stress is formed during the MCT loading condition as attached ice and wind result in additional conductor stressing. These three different creeps are compared and the largest is used to describe the overall plastic deformation of the conductor [30]. These computations employ either the creep-strain curves produced by experimental measurements when novel conductors are used, or the model equations for the more traditional conductor types [28]. These ageing computations are performed iteratively yielding more realistic results, since the stress is reduced with time as the creep-strain increases.

#### **2.4. Final System Conditions**

After performing the ageing computations, the plastic elongation is converted into the equivalent thermal elongation. The latter is defined by the difference in conductor temperature that results in the same increase in conductor length as the increase caused by the plastic deformation of the conductor. This is transformed into the tension difference that is required to negate the sag resulting from the conductor plastic elongation. This correction is then used in the mechanical computation level and since the initial conditions of the system have changed, the new plastic elongation is calculated again. This procedure is repeated until total negation of creep occurs or limitations of the system do not allow further increase in conductor initial tension. Once this iterative process is completed the final system conditions of a particular conductor on a given structure are known. These are the conductor ampacity, conductor sag with creep, and conductor sag when creep is negated as well as the initial over-tension required to negate the creep.

### **3. Performance of Different Conductor Technologies**

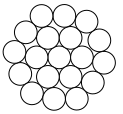
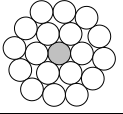
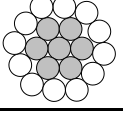
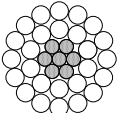
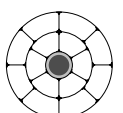
Results from the application of this methodology for the comparison of the performance of different conductor technologies on the same pre-specified OHL system for different conditions are presented, illustrating how conductor properties define the choice of an optimum conductor. Additionally, an investigation of how different materials (i.e. steel and aluminium) alter conductors' performance is performed.

#### **3.1. System Description**

The structure considered in this study is a single circuit 33 kV wood pole distribution line with ruling span of 110 m. This structure is considered as a 10 m stout wood with planting depth of 1.5 m [31]. The conductor attaching points are located at 8.3 m above the ground level allowing 3.1 m of maximum sag [32]. The mechanical strength of this structure is defined by the insulator pin which has a 70 kN tension failing load. The overall structure meets the requirements of [20].

The weather conditions at the location of the OHL are considered as part of the system since they influence the MCT and safety factors. For this study a “normal” altitude loading is assumed, with combined wind of  $380 \text{ N/m}^2$  and ice of 9.5 mm radial thickness and  $913 \text{ kg/m}^3$  density at  $-5.6 \text{ }^\circ\text{C}$  [20-21, 32-33]. The everyday operating conditions are set to vibration limit of 20% RBS for aluminium conductors at the temperature of  $+5 \text{ }^\circ\text{C}$ . Ambient temperature for the electrical calculations is set to  $40 \text{ }^\circ\text{C}$ .

Table 1 illustrates the five different conductor types investigated within this study. The distinction of ACSRs between soft and hard is essential due to the influence of the steel content on conductor RBS, resistance, modulus of elasticity, coefficient of thermal expansion and weight which make similar cross-sectional conductors behave differently on the system. The ACCR and ACCC with trapezoidal wires (ACCC/TW) are novel composite conductors with HTLS performance [2-3].

Bare conductor type	Core strands shape & material	Outer strands shape & material	Conductor Schematic
All aluminium alloy conductor ( <b>AAAC</b> )	Cylindrical aluminium alloy (6201-T81) with 53% IACS* conductivity (AL3)	Cylindrical aluminium alloy (6201-T81) with 53% IACS* conductivity (AL3)	
Aluminium conductor steel reinforced – 1:1.8 steel to aluminium ( <b>soft ACSR</b> )	Cylindrical steel with 9% IACS* conductivity	Cylindrical aluminium alloy (1350-H19) with 61% IACS* conductivity (AL1)	
Aluminium conductor steel reinforced – 1:1.7 steel to aluminium ( <b>hard ACSR</b> )	Cylindrical steel with 9% IACS* conductivity	Cylindrical aluminium alloy (1350-H19) with 61% IACS* conductivity (AL1)	
Aluminium conductor composite reinforced ( <b>ACCR</b> )	Cylindrical metal matrix composite wires with alumina fibers with 23-24% IACS conductivity [2]	Cylindrical aluminium-zirconium alloy with 61% IACS* conductivity [2]	
Aluminium conductor composite core / trapezoidal wire ( <b>ACCC/TW</b> )	Solid cylindrical core of a hybrid non-conductive polymer matrix with both carbon and glass fibers [3]	Trapezoidal of fully annealed (O') tempered aluminium alloy (1350-H0) with 63% IACS* conductivity [3]	

\* International Annealed Copper Standards

Table 1

### 3.2. Mechanical Performance of Different Conductors

#### 3.2.1. Zones of Sag

The mechanical performance of conductors of different sizes on the OHL structure is influenced by the three limitations described within the mechanical computations. Fig. 2

illustrates the sag performance of different radius AAAC conductors at maximum weather loading and maximum electrical loading (set at 70 °C) conditions. As already mentioned the ‘sag zones’ were introduced in [10]. Here another case study of their application on a different OHL system is presented including more AAAC conductors with and without creep and later extending their interpretation based on various conductor properties.

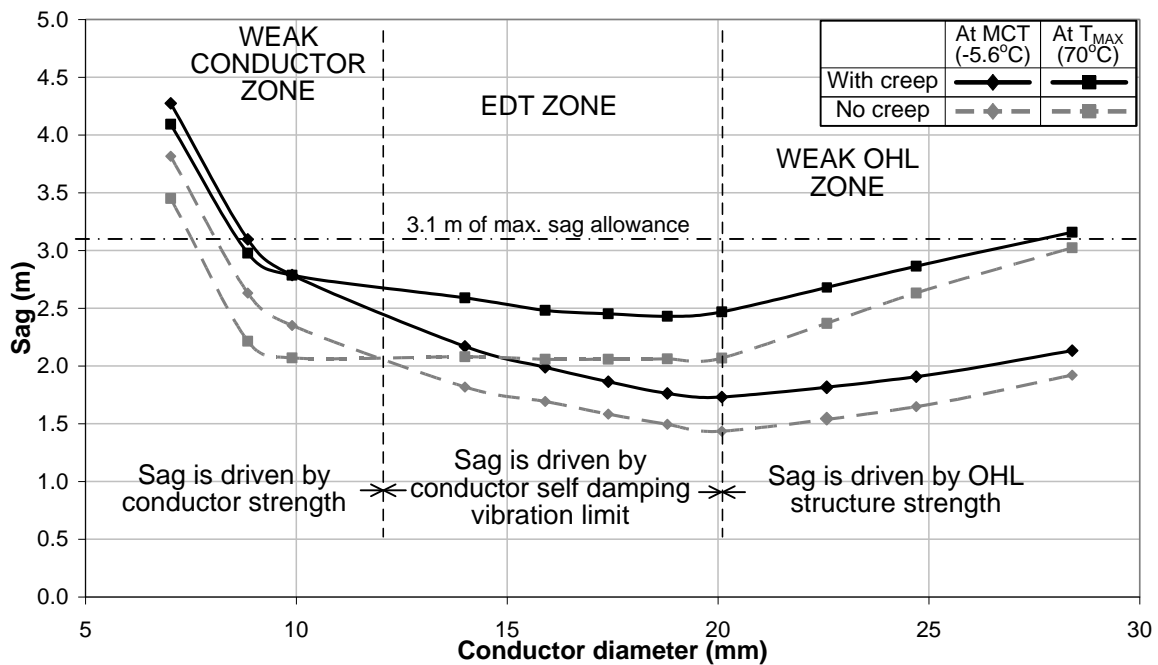


Figure 2

The three sag zones are defined as follows:

*Weak conductor zone:* The low conductor strength is the main reason for the excessive sag. Within this zone the conductor sag at maximum weather loading is larger than that at maximum electrical loading. This is due to the larger elastic elongation caused by the additional weight on the conductor compared to the thermal elongation caused by the current flow within the conductor. In addition, the plastic deformation of these conductors is governed by the MCT at weather loading and not by the long term creep.

*EDT zone:* Sag is driven by the conductor self damping vibration limit. This is usually set as a percentage of RBS and therefore the homogeneous conductors (like the AAACs illustrated in Fig. 2) - or conductors with constant core to outer strands ratio - within this zone are expected to have similar sag values. The mechanical performance of conductors of these sizes can be further improved using vibration dampers and thus increasing the EDT of the vibration limit which is usually 20% RBS. The creep effect of these conductors is governed by the long term creep.

*Weak OHL zone:* Further increase in conductor size results only in an increase of conductor weight (and not in tension) as MCT is limited by the strength of the OHL structure, which in turn reduces the system's EDT. This results in increased sag values with increased conductor size, as increase of the conductor's weight stresses the conductor further causing more elastic elongation. The creep strain for these conductors is also governed by long term creep; however, since the EDT is reduced compared to the previous zone, the creep is lower.

It should be noted that the results without creep are obtained when the creep strain is negated by including an initial over-tension during the conductor installation while the results with creep consider 10 years of conductor plastic elongation and assume a total duration of 500 hours for maximum weather loading. This duration is essential to compute the creep caused by the conductor's maximum mechanical loading, particularly for the small conductor sizes within the weak conductor zone, as these conductors are

affected more by the maximum weather loading and its duration [30]. The elevated temperature creep effect is not considered at 70 °C [34].

Fig. 3 illustrates the sag zones of the different conductors erected on the OHL structure described previously and demonstrates how these are influenced by the system, the conductor type, and the OHL structure. Novel composite conductors of smaller sizes have not (yet) been produced by the manufactures and therefore only one boundary is illustrated for these conductors. It is important to emphasise that the RBS of ACCC/TW is computed by considering only the composite core and totally neglecting the aluminium strands [3] while in all other conductor types the RBS is the result of the whole conductor (i.e. combining the strength of core and outer strands).

The EDT zone is reduced as the strength of conductor material(s) is increased; the arrows illustrate the shift of the boundaries of this zone for the different conductor types. In particular, by observing the boundaries one can tell which conductor is the strongest. Consequently, it can be seen that the AAACs are weaker than the hard ACSRs since the latter have smaller EDT zone. In contrast to the hard ACSRs, the soft ones are weaker than the AAAC conductors forming wider EDT zone. The slope of increase in sag within the weak OHL zone is the same for all the conductors since the OHL strength governs their mechanical performance (sag). Another important observation that can be derived from the sag zones is that the conductor with the best electro-mechanical performance is the one with size closed to the boundary of EDT and weak OHL zones. However, if the ground clearance permitted by the structure allows the installation of a larger conductor

then this will reduce the mechanical performance but increase the electrical performance of the system.

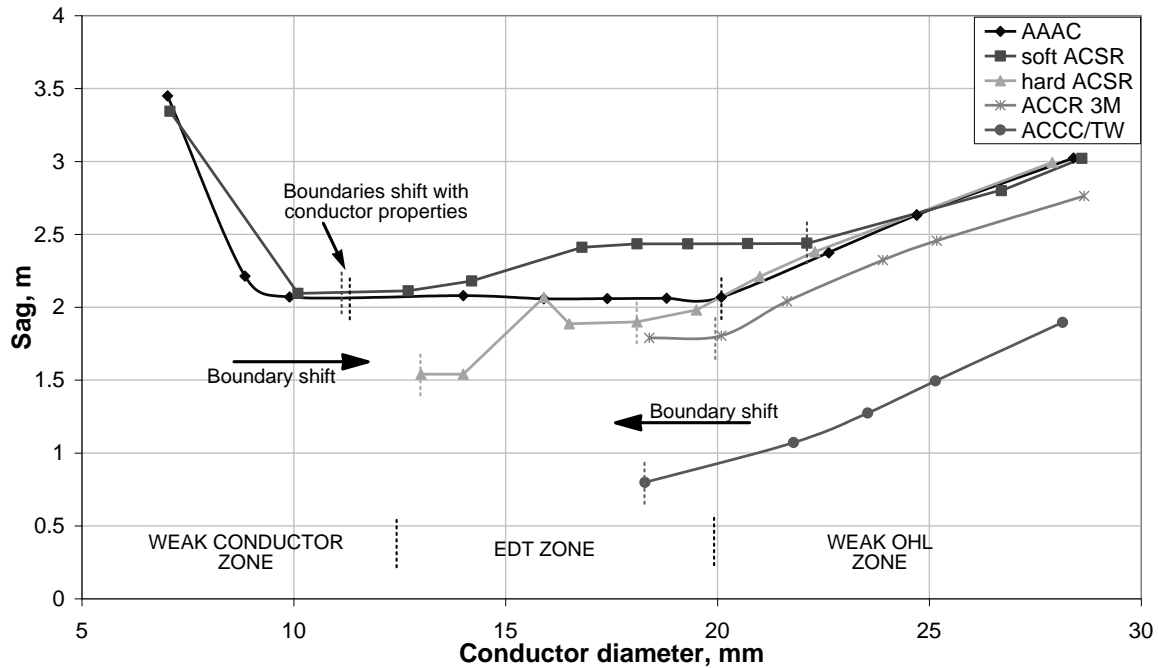


Figure 3

### 3.2.2. Critical Conductor Properties

Fig. 4 compares the sag performance of the different conductor types of Table 1 during the maximum electrical loading conditions (70 °C) considering plastic elongation. It also shows the effect of an increase in modulus of elasticity ( $E$ ) of conductor composition as well as a reduction in the coefficient of thermal expansion ( $\epsilon$ ). The modulus of elasticity and coefficient of thermal expansion for bi-material conductors were derived by using equations (2) and (3). The cross-sectional areas ( $A$ ) of the different conductors were derived by using the standards for the common conductors, and technical notebooks and relevant literature for the ACCRs and ACCC/TW respectively [2-3, 17-18, 35-36].



$$E_{TOT} = \frac{E_a \cdot m + E_b}{m + 1} \quad (2) \quad \varepsilon_{TOT} = \frac{\varepsilon_a \cdot E_a \cdot m + \varepsilon_b \cdot E_b}{m \cdot E_a + E_b} \quad (3)$$

where:  $m = \frac{A_a}{A_b}$  and  $a, b$  define different materials.

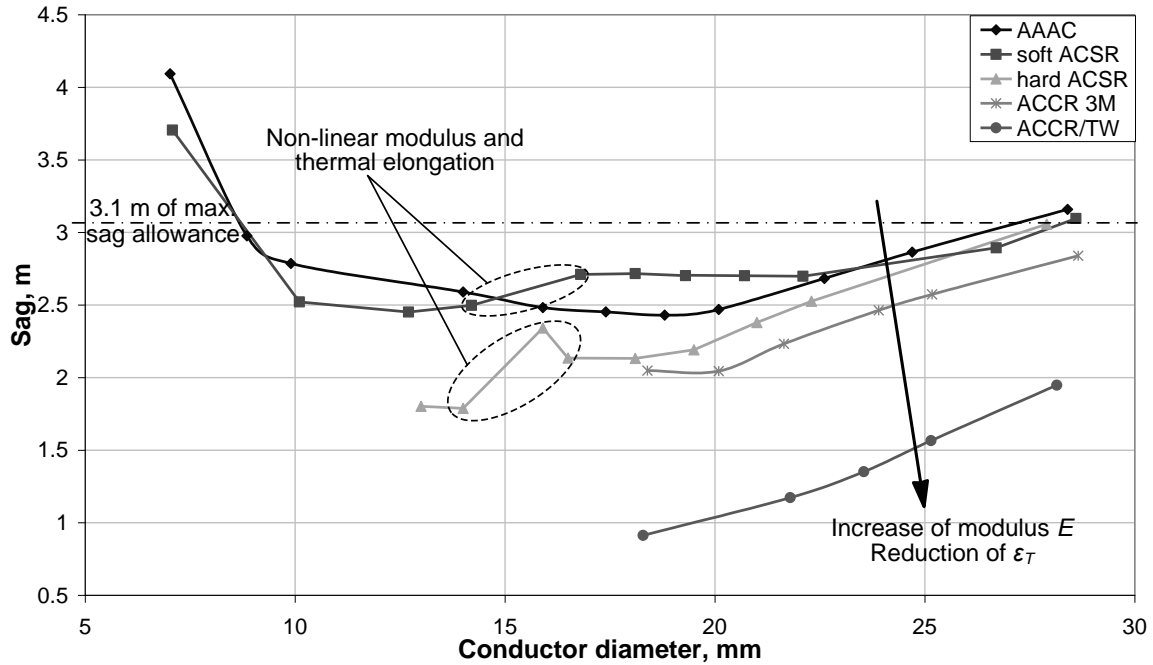


Figure 4

ACSR conductors present non-linear changes in modulus and thermal elongation along the range of the different sizes. These anomalies are more intense for the smaller conductors within the EDT zone and affect considerably their sag performance (Fig. 4). They are caused by stranding pattern changes at the different conductor sizes which drastically alter the steel-to-aluminium content for both the soft and hard ACSRs. Such anomalies are not present for homogeneous conductors like the AAACs. Furthermore, the ACCR and ACCC/TW composite conductors are designed to have small variation in core-to-conductor ratio permitting a more uniform sag performance.

When the sag performance of different conductor types is compared, it can be seen that an increase in elastic modulus and reduction in the coefficient of thermal expansion

results in sag mitigation. ACCC/TWs develop the smallest sag values, which illustrates the very low thermal elongation factor of their composite core when compared to other conductor types [3]. ACCRs have the second best performance.

ACCC/TWs are lighter compared to hard ACSR of equivalent diameter but heavier than the AAACs and soft ACSR as the trapezoidal shape wires increase the amount of aluminium for the same conductor outer diameter [10]. Hence, the approximately 16% heavier ACCC/TW sags much less than the AAAC and soft ACSR of similar diameter. Their sag performance at maximum electrical loading conditions (70 °C) is also better than the performance of ACCRs. However, the large difference of thermal expansion coefficient between the composite core and aluminium strands for the ACCC/TW increases the risk of developing bird cages (i.e. the separation of the outer conductor strands from the core) in long spans with loss of structural integrity, at very high operating temperatures [3, 37].

### **3.3. Electrical Performance: Ampacity & Losses**

By increasing the conductor diameter the current capacity is increased, raising the maximum power rating of the OHL. The maximum conductor diameter size, though, is limited by the permitted sag on the particular system. For this reason, in the example of the system studied here, the conductors above the dotted lines of Fig. 4 could not be used for re-conductoring. Fig. 5 illustrates the exact ampacities for the different conductors at 70 °C, by their total cross-sectional area ( $A$ ), diameter and weight. The changes in steel-to-aluminium ratio over the range of sizes of the soft and hard ACSR also affect their

electrical performance. In contrast, the uniform conductors have a linear increase of ampacity with the increase in conductor diameter.

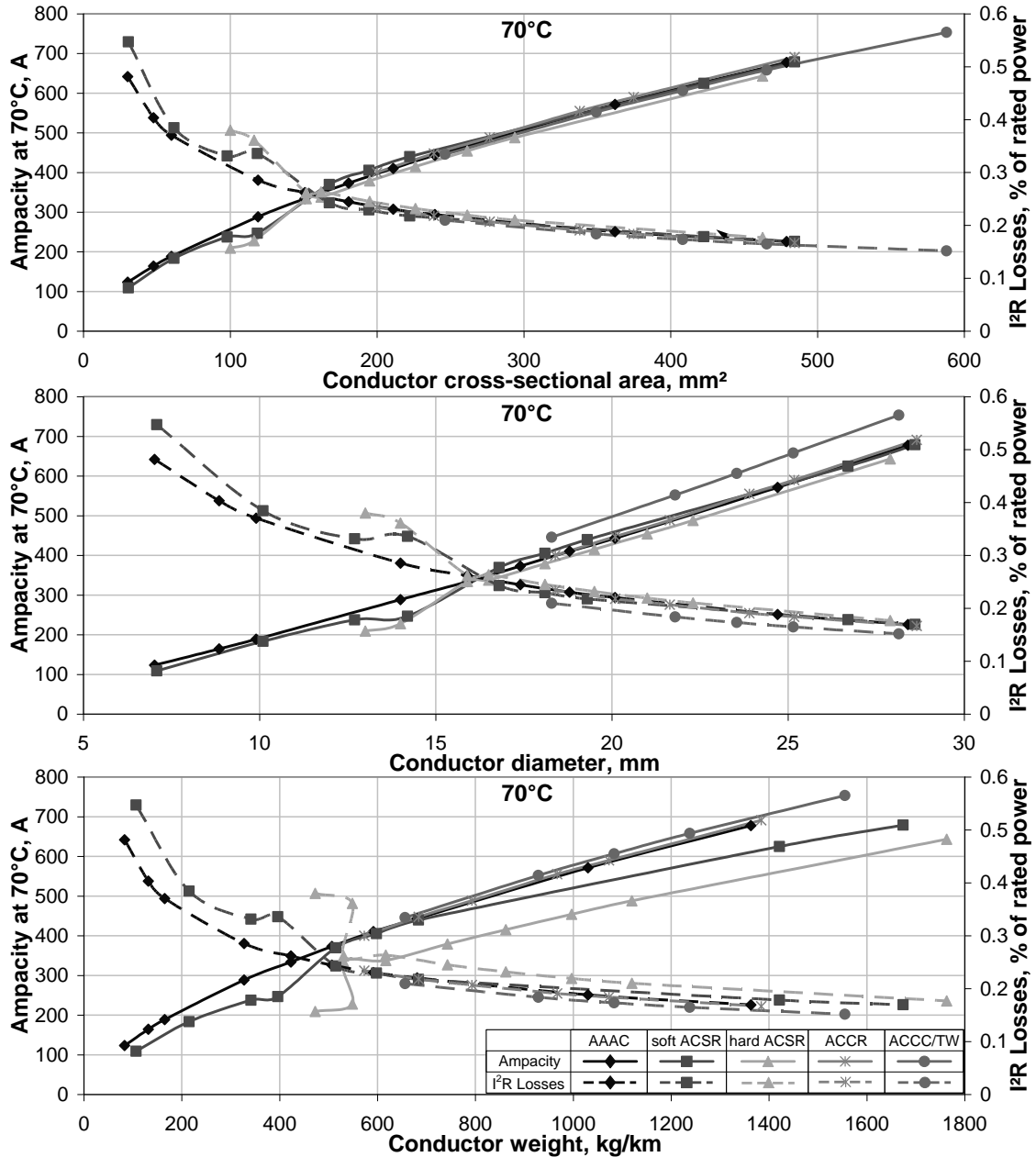


Figure 5

The ampacities of the different conductor types are very similar when compared based on their cross-sectional area, however, the hard ACSRs have 10 A to 20 A lower ampacity

than the equivalent conductors of other types and develop more  $I^2R$  losses. This is the result of their larger volume resistivity compared to the soft ACSRs and AAACs, and their steel core losses which are introduced by the increased steel content when compared to soft ACSR [38]. Another important observation regards the lower losses of the ACCC/TW conductors when compared with the equivalent in diameter aluminium based conductors (i.e. AAACs and ACCRs) considering that their composite core is a non-conductive compound. This is due to the trapezoidal aluminium strands.

Finally, when the electrical performance of the conductors is compared based on their weight the poor performance of the ACSR conductors is obvious and more noticeable for the hard ones. On the other hand, the ACCC/TWs appear to have the best performance. The comparison of the conductors in respect to their electrical performance based on their weight is considered to be the most informative one, since weight also defines the maximum conductor size that can be installed on the system.

### **3.3. Holistic (Electro-Mechanical) Comparison of Equivalent Weight Conductors**

Given the previous results, Fig. 6 shows further comparisons of conventional AAAC conductors and equivalent weight novel conductors at different  $T_{MAX}$  in respect to their electrical performance on this system.

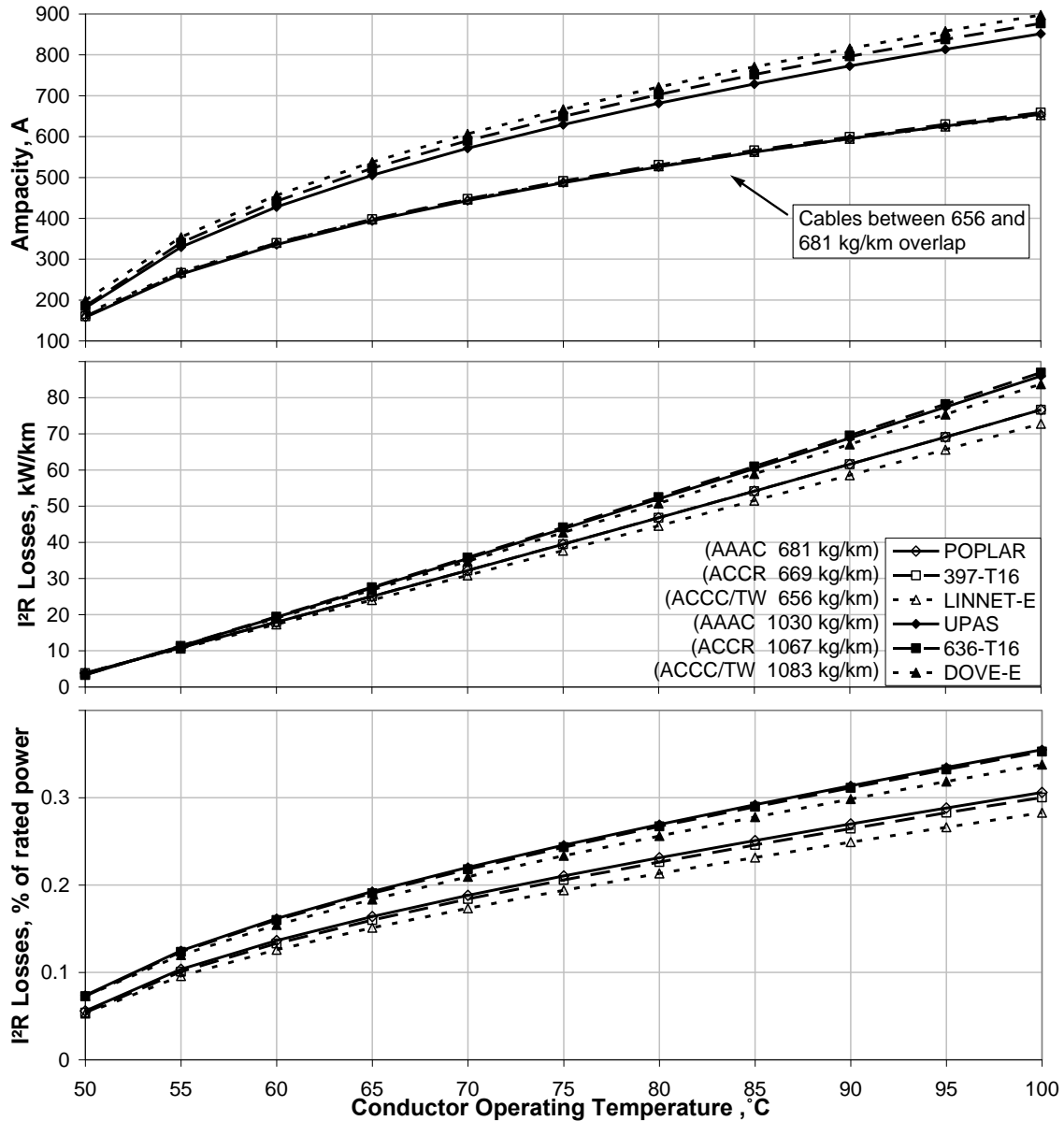


Figure 6

The comparison of the heavier conductors (362-L3 (Upas), 636-T16, and Dove-E) indicates that the ACCC/TW allows more ampacity than the equivalent weight ACCR and AAAC and produces lower losses (Fig. 6). In contrast, comparison of lighter conductors (Linnet-E, 239-AL3 (Poplar) and 397-T16) shows that they have almost identical ampacities. However, the ACCC/TW conductor appears to have lower losses,

particularly at higher temperatures (i.e. 1.6 and 3 kW/km at 70 °C and 90 °C, respectively, when compared to the Poplar) indicating their lower resistance. Their normalised losses to the maximum power rating appear to have 5% difference at 70 °C which further increases to 10% at 90 °C in favour of the ACCC/TW's performance.

It should be noted that even though ACCC/TWs may operate at higher temperatures allowing greater ampacities, the analysis for this paper focuses on their operation at lower temperatures to keep their losses to values similar to conventional conductors.

The mechanical performance of the same conductors is compared in Fig. 7 for different OHL span lengths at 70 °C. Fig. 7, in combination with previous results (Figs 3 and 4), indicates that when the equivalent weight conductors are compared, the increase in sag caused by the increase in span length is steeper for those with smaller modulus and larger thermal elongation (see difference in the slopes of the lines for Linet-E compared to Poplar and 397-T16). Furthermore, the comparison of conductors of the same technology based on their weight (Fig. 7) highlights the weight effect on sag, given by the steeper increase in sag for the heavier conductors. This demonstrates the importance of the implementation of lightweight conductor technologies particularly at weak wood pole OHL structures.

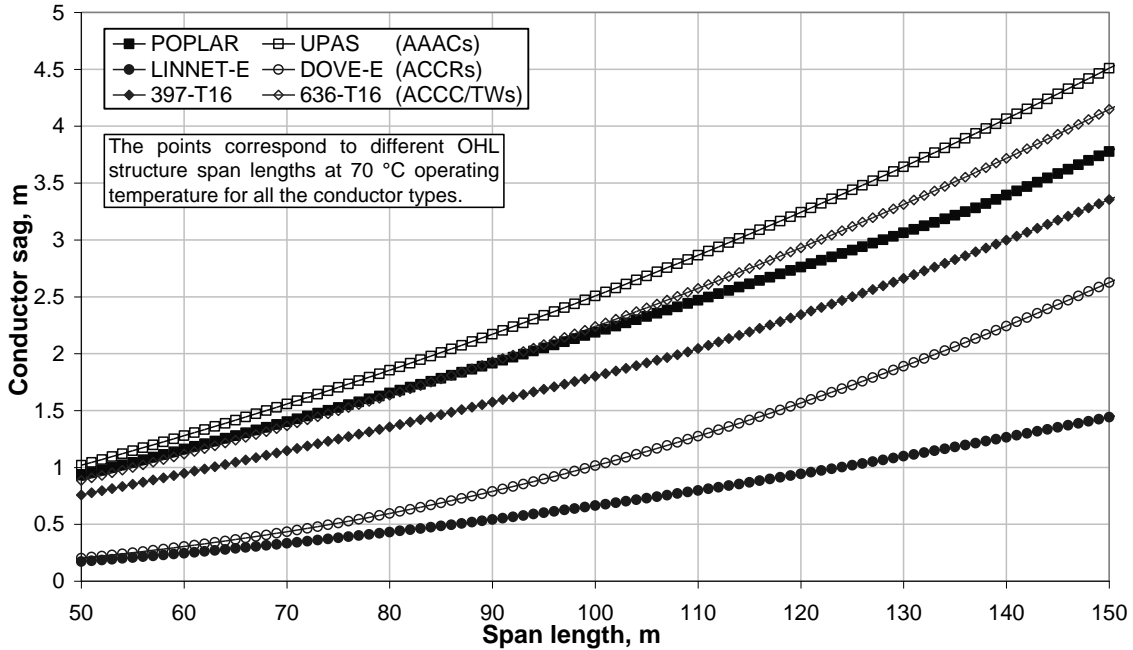


Figure 7

In order to show the holistic performance of these conductors on the same structure their combined sag and ampacity coordinates at different operating temperatures are plotted in Fig. 8. It can be seen that the novel composite conductors allow higher ampacities with lower sag values. Further increase in ampacity can be achieved by further increase in their  $T_{MAX}$  (e.g. above 90 °C) or by re-conductoring with larger sizes and operate at the normal  $T_{MAX}$  (70 °C). The second approach reduces the losses of the system as well (Fig. 6).

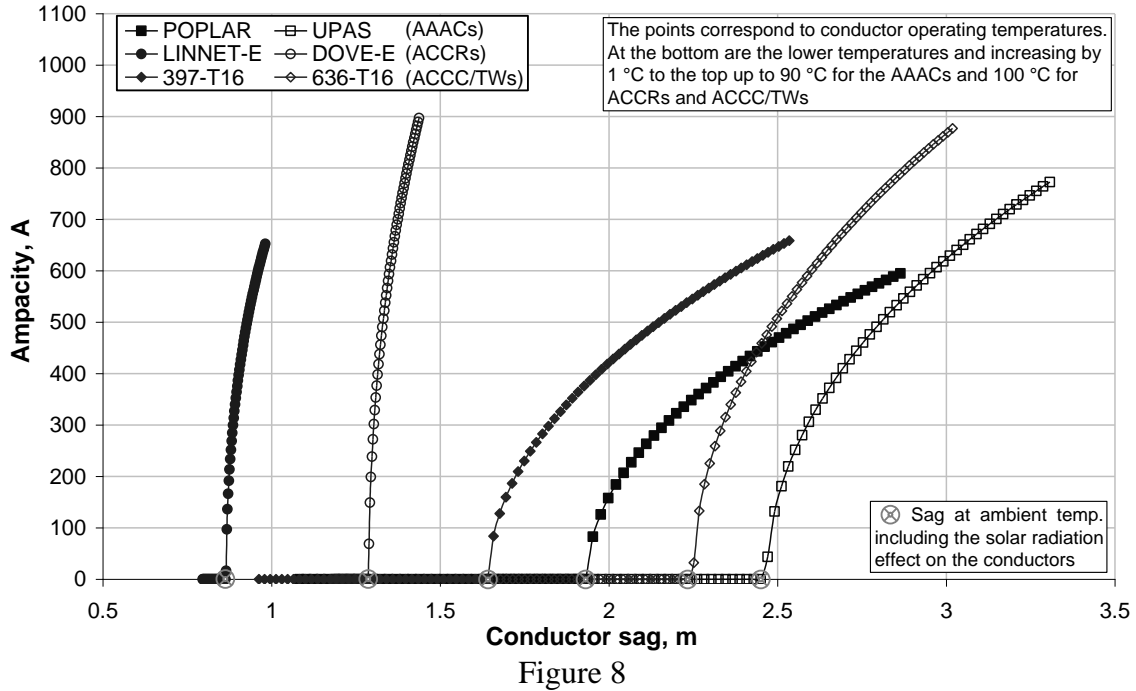


Fig. 8 also shows that there is no elevated temperature creep effect in the 10 years of operation for the AAACs, since it is assumed that for this particular 33 kV OHL system the conductor would operate at  $T_{MAX}$  for less than 500 hours. However, if the duration of the elevated temperature operation is increased for this system then the sag for the conventional AAAC conductors will increase.

The lower sag values for the novel HTLS conductors, particularly for the ACCC/TW, allows an increase in the planting depth of the pole, therefore increasing the structure's strength and allowing larger (weight) span lengths [31].

Finally, the low sag levels observed for the ACCC/TW conductors (like the two presented in Fig. 8) offer the additional option of upgrading the 33 kV structure to 66 kV without infringing the required 6.0 m minimum clearance to ground [21, 39]. In other



words, when the 33 kV structure with a conventional conductor is re-conducted with an equivalent in weight ACCC/TW the ground clearance is increased by approximately 1 m when the creep is negated (Fig. 3). This increases further to 1.5 m when the AAAC is not initially over-tensioned for the required creep negation (Fig. 8). It is important to emphasize that this conductor develops larger sag values during the maximum weather loading.

#### **4. Conclusions**

The comparative study of the different conductors on this 33 kV OHL structure, firstly shows that from the conventional conductors the AAACs have better electrical and mechanical performance, particularly when initial over-stressing is applied to negate the creep-strain effect. AAACs have better ampacity-to-weight ratio, thus they stress the OHL structure less, which potentially allows re-conducting with larger conductors without the need of structure and foundation reinforcement. Soft ACSRs are in general heavier than the AAACs and consequently impractical for the comparatively weak wood pole structures, although their electrical performance is not very different. Hard ACSRs are very heavy and thus unsuitable for most wood pole applications.

Another substantial finding involves the new composite HTLS conductors which can increase the power transfer of the 33 kV wood pole system either through increased operating temperatures or re-conducting with larger conductors. ACCC/TW conductors have very low sag values, as a result of the very low thermal expansion coefficient and density as well as a high modulus of elasticity. This allows the following options, or combination of them, for improving system performance:

- Increasing the span length of the structure and hence reducing the number of poles needed.
- Reducing the height of the structure requirements or increasing the planting depth and therefore the structure's strength particularly in "weak" ground.
- Increasing the maximum operating temperature of the conductor.
- Re-conductoring with larger conductors.
- Increasing the voltage level of the OHL structure to 66 kV.

The last three points increase the power capacity of the structure with minimum structural changes, while the last two reduce the losses as well.

As a concluding remark, an 'ideal' conductor for operation at normal operating temperatures on weak structure systems can be identified based on conductors' properties and their effect on system's performance, as reported in this paper. Such a conductor would have low density strength member, high strength and low coefficient of thermal expansion combined with high compaction and low resistance-to-weight soft outer strands. This design could offer potential benefits for the performance of relatively weak wood pole structures, such as the one investigated here.

### **Acknowledgment**

This work is funded through the EPSRC Supergen V, UK Energy Infrastructure (AMPerES) grant in collaboration with UK electricity network operators working under Ofgem's Innovation Funding Incentive scheme; - full details on <http://www.supergen-amperes.org>

## References

- [1] IEC 61597: Overhead Electrical Conductors - Calculation Methods for Stranded Bare Conductors. International Electrotechnical Commission. May 1995.
- [2] 3M. Aluminum Conductor Composite Reinforced Technical Notebook (477 kcmil family) Conductor & Accessory Testing, 2006: Available from: [http://www.energy.ca.gov/2004\\_policy\\_update/documents/2004-06-14-workshop/public\\_comments/2004-06-28\\_3M\\_PART2.PDF](http://www.energy.ca.gov/2004_policy_update/documents/2004-06-14-workshop/public_comments/2004-06-28_3M_PART2.PDF).
- [3] Alawar A, Bosze EJ, Nutt SR. A composite core conductor for low sag at high temperatures. IEEE Transactions on Power Delivery. 2005;20(3): 2193-9.
- [4] Zamora I, Mazon AJ, Eguia P, Criado R, Alonso C, Iglesias J, et al., editors. High-temperature conductors: a solution in the uprating of overhead transmission lines. IEEE Power Tech Proceedings, Porto-Portugal; 2001.
- [5] Shankle DF. Incremental Voltage Uprating of Transmission Lines. IEEE Transactions on Power Apparatus and Systems. 1971;PAS-90(4): 1791-5.
- [6] Albizu I, Mazon AJ, Zamora I, editors. Methods for increasing the rating of overhead lines. Power Tech, 2005 IEEE Russia; 2005.
- [7] Kotaka S, Itou H, Matsuura T, Yonezawa K, Morikawa H. Applications of Gap-type Small-Sag Conductors for Overhead Transmission Lines. SEI Technical Review. [SEI Technical Review]. Jun. 2000(SEI Technical Review, No 50): 64-72.
- [8] Adams HW. Steel Supported Aluminum Conductors (SSAC) for Overhead Transmission Lines. IEEE Transactions on Power Apparatus and Systems. 1974;PAS-93(5): 1700-5.
- [9] Exposito AG, Santos JR, Cruz Romero P. Planning and Operational Issues Arising From the Widespread Use of HTLS Conductors. IEEE Transactions on Power Systems. 2007;22(4): 1446-55.
- [10] Kopsidas K, Rowland SM. A Performance Analysis of Reconductoring an Overhead Line Structure. IEEE Transactions on Power Delivery. 2009;24(4): 2248-56.
- [11] Kopsidas K. Modelling Thermal Rating of Arbitrary Overhead Line Systems [PhD Thesis]. Manchester, UK: The University of Manchester; 2009.
- [12] Kopsidas K, Rowland SM. A Holistic Method for a Conductor's Ampacity and Sag Computation on an OHL Structure. IEEE Transactions on Power Delivery. under review.
- [13] BS EN 50182: Conductors for Overhead Lines - Round Wire Concentric Lay Stranded Conductors. British Standards. 2001.
- [14] CIGRE SC.B2 - WG.B2.12: Sag-Tension Calculation Methods for Overhead Lines. 2007.
- [15] ASTM B 193-02: Test Method for Resistivity of Electrical Conductor Materials. Annual Book of ASTM Standards. 2005;02.03: 68-72.
- [16] ASTM B 230/B 230M-99: Specification for Aluminum 1350-H19 Wire for Electrical Purposes. Annual Book of ASTM Standards. 2005;02.03: 91-4.
- [17] ASTM B 498/B 498M-98(2002): Specification for Zinc-Coated (Galvanized) Steel Core Wire for Aluminum Conductors, Steel Reinforced (ACSR). Annual Book of ASTM Standards. 2005;02.03: 218-21.

- [18] ASTM B 779 - 03: Standard Specification for Shaped Wire Compact Concentric-Law-Stranded Aluminum Conductors, Steel Reinforced (ACSR/TW). Annual Book of ASTM Standards. 2005;02.03: 309-14.
- [19] ASTM B232/B 232M-01: Specification for Concentric-Lay-Stranded Aluminum Conductors, Coated-Steel Reinforced (ACSR). Annual Book of ASTM Standards. 2005: 106-21.
- [20] ENATS 43-40: Single Circuit Overhead Lines on Wood Poles for Use at High Voltage Up to and Including 33kV. Energy Networks Association Technical Specifications. Issue 2, 2004(2).
- [21] BS EN 50341-3: Overhead electrical lines exceeding AC 45 kV - Part 3: Set of National Normative Aspects. British Standards. 2001.
- [22] Dwight HB. Skin Effect in Tubular and Flat Conductors. AIEE Transactions. 1918;37: 1379-403.
- [23] Lewis WA, Tuttle PD. The Resistance and Reactance of Aluminum Conductors, Steel Reinforced. AIEE Transactions. 1959;77(3): 1189-215.
- [24] Olver FWJ. 9. Bessel Functions of Integer Order. In: Abramowitz M, Stegun IA, editors. Handbook of Mathematical Functions. Washington, D. C.: U. S. Dept. Commerce; 1964. p. 378-85.
- [25] Howington BS, Rathbun LS. AC Resistance of ACSR - Magnetic and Temperature Effects. IEEE Transactions on Power Apparatus and Systems. 1985;PAS-104(6): 1578-84.
- [26] Kirkpatrick L, (Ed.). Aluminum Electrical Conductor Handbook. Third ed. Washington, D.C.: the Aluminum Association; 1989.
- [27] IEEE Standard for Calculating the Current-Temperature of Bare Overhead Conductors. IEEE Std 738-2006 (Revision of IEEE Std 738-1993). 2007: 1-59.
- [28] Harvey JR, Larson RE. Creep Equations of Conductors for Sag-Tension Calculations. IEEE/PES Winter Meeting Conference. Paper No. C71 190-2, 1972.
- [29] Harvey JR, Larson RE. Use of Elevated-Temperature Creep Data in Sag-Tension Calculations. IEEE Transactions on Power Apparatus and Systems. 1970;PAS-89, No 3: 380-6.
- [30] CIGRE SC22 - WG05: Permanent elongation of conductors. Predictor equation and evaluation methods. *Electra* N° 75. 1981: 63-98.
- [31] BS 1990-1: Wood poles for overhead power and telecommunication lines - Part 1: Specification for soft wood poles. British Standards. 1984.
- [32] BS EN 50423-3: Overhead electrical lines exceeding AC 1 kV up to and including AC 45 kV - Part 3: Set of National Normative Aspects. British Standards. 2005.
- [33] BS EN 50423-1: Overhead electrical lines exceeding AC 1 kV up to and including AC 45 kV - Part 1: General requirements - Common specifications. British Standards. 2005.
- [34] IEEE Guide for Determining the Effects of High-Temperature Operation on Conductors, Connectors, and Accessories. IEEE Std 1283-2004. 2005: 1-28.
- [35] Development of Stress-strain Polynomials and Creep Parameters for ACCC/TW Conductors, 2008 Jul. 12: Available from: [www.powline.com/files/cables/ctc\\_conductors.pdf](http://www.powline.com/files/cables/ctc_conductors.pdf).

- [36] ASTM B 398/B 398M-02: Standard Specification for Aluminum-Alloy 6201-T81 Wire for Electrical Purposes. Annual Book of ASTM Standards. 2005;02.03: 178-81.
- [37] Nigol O, Barrett JS. Characteristics of ACSR Conductors at High Temperatures and Stresses. IEEE Transactions on Power Apparatus and Systems. 1981;PAS-100(2): 485-93.
- [38] Morgan VT, editor. Electrical Characteristics of Steel-Cored Aluminium Conductors. IEEE Proceedings; Feb. 1965; London.
- [39] BS EN 50341-1: Overhead electrical lines exceeding AC 45 kV - Part 1: General requirements - Common specifications. British Standards. 2001.

### **List of Table & Figures Captions**

Table 1: Properties of the different types of conductors studied.

Figure 1: Summary flowchart for the methodology for sag and ampacity calculations.

Figure 2: AAAC sag performance at maximum designed weather loading and operating temperature.

Figure 3: Sag zones of different conductor types at 70 °C without creep.

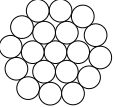
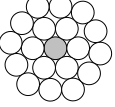
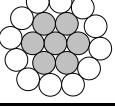
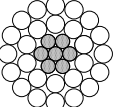
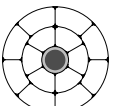
Figure 4: Sag performance of different conductor types at 70 °C including creep.

Figure 5: Electrical performance of different conductor types.

Figure 6: Electrical performance of conductors of similar-weight at different maximum operating temperatures.

Figure 7: Sag performance of different type but similar-weight conductors for different spans.

Figure 8: Plots of sag and ampacity of similar-weight conductors at different operating temperatures.

Bare Conductor Type	Core strands shape & material	Outer strands shape & material	Conductor Schematic
All aluminium alloy conductor ( <b>AAAC</b> )	Cylindrical aluminium alloy (6201-T81) with 53% IACS* conductivity (AL3)	Cylindrical aluminium alloy (6201-T81) with 53% IACS* conductivity (AL3)	
Aluminium conductor steel reinforced – 1:18 steel to aluminium ( <b>soft ACSR</b> )	Cylindrical steel with 9% IACS* conductivity	Cylindrical aluminium alloy (1350-H19) with 61% IACS* conductivity (AL1)	
Aluminium conductor steel reinforced –1:1.7 steel to aluminium ( <b>hard ACSR</b> )	Cylindrical steel with 9% IACS* conductivity	Cylindrical aluminium alloy (1350-H19) with 61% IACS* conductivity (AL1)	
Aluminium conductor composite reinforced ( <b>ACCR</b> )	Cylindrical metal matrix composite wires with alumina fibers with 23-24% IACS conductivity [2]	Cylindrical aluminium-zirconium alloy with 61% IACS* conductivity [2]	
Aluminium conductor composite core / trapezoidal wire ( <b>ACCC/TW</b> )	Solid cylindrical core of a hybrid non-conductive polymer matrix with both carbon and glass fibers [3]	Trapezoidal of fully annealed (O') tempered aluminium alloy (1350-H0) with 63% IACS* conductivity [3]	

\* International Annealed Copper Standards

Table 1

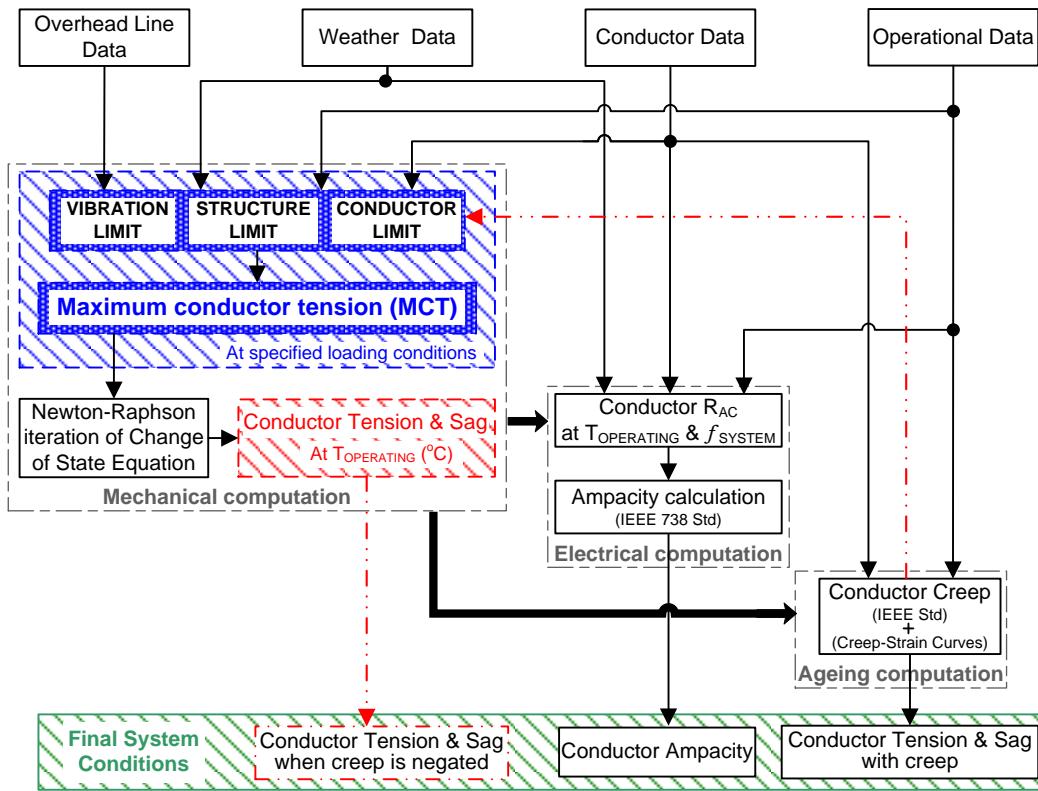


Figure 1

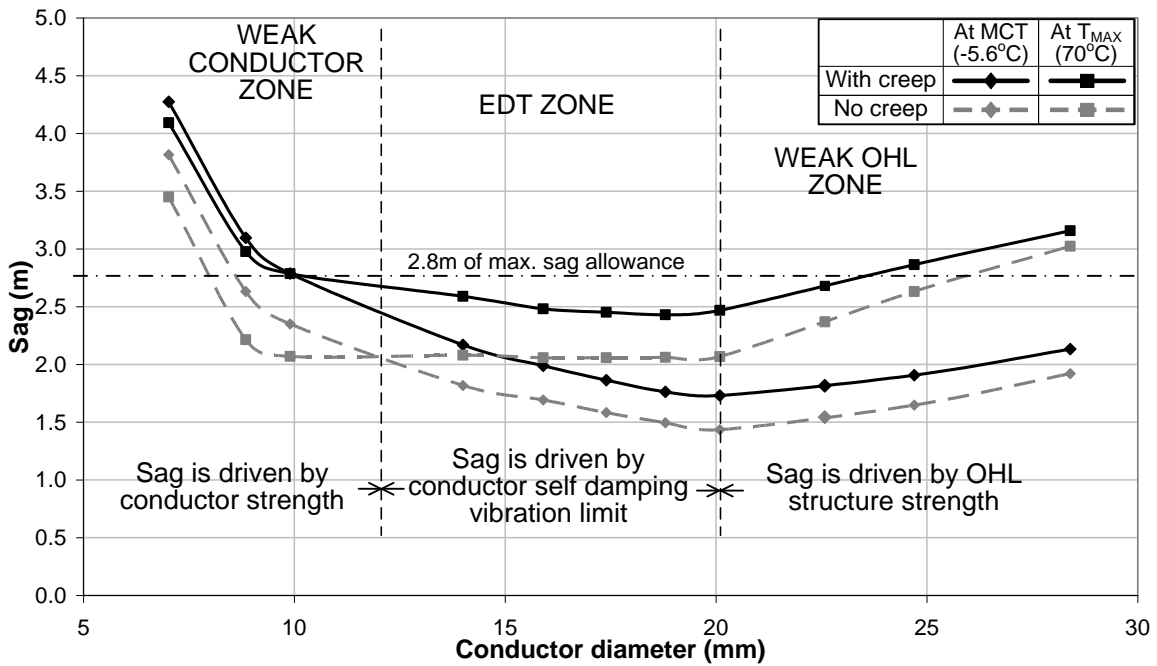


Figure 2

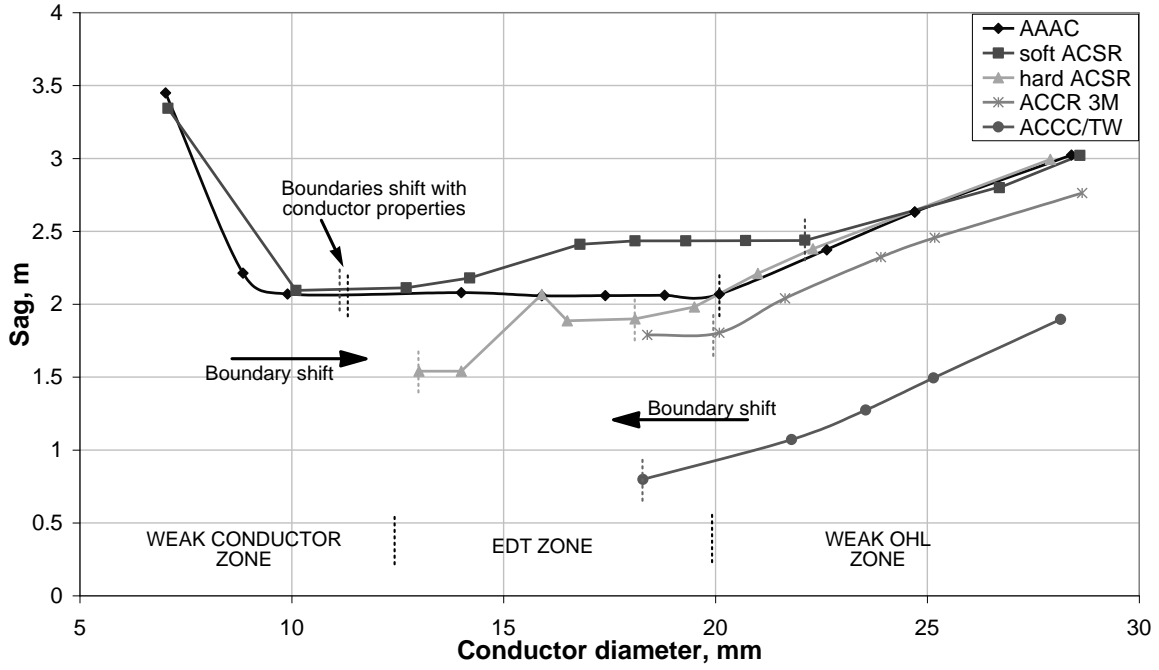


Figure 3

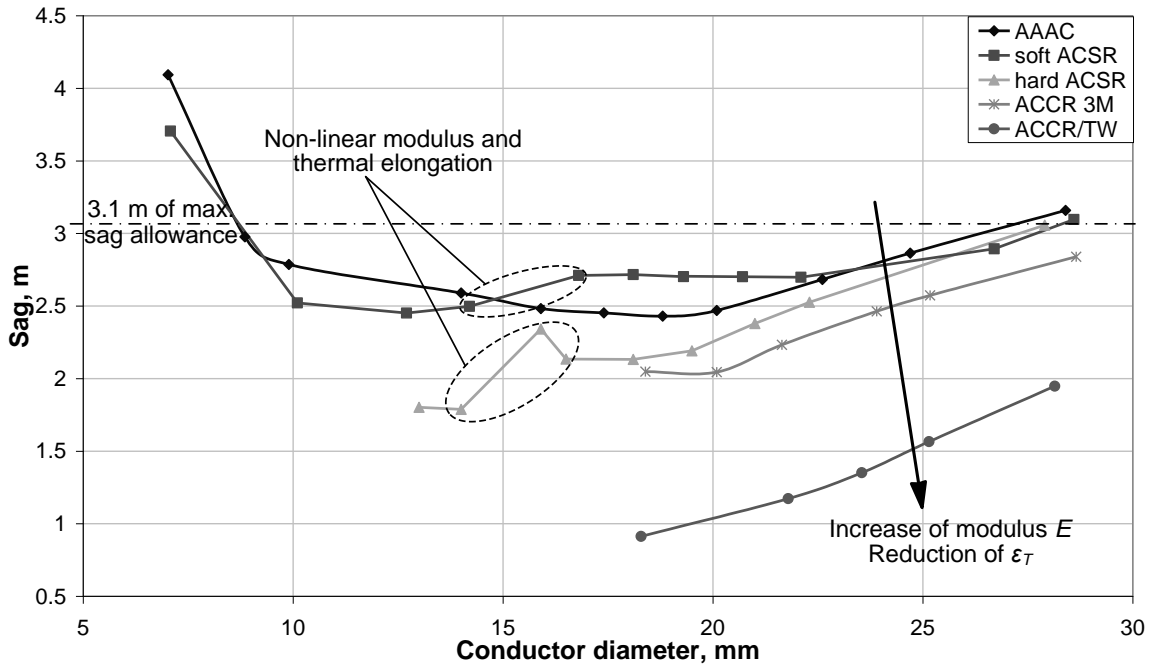


Figure 4



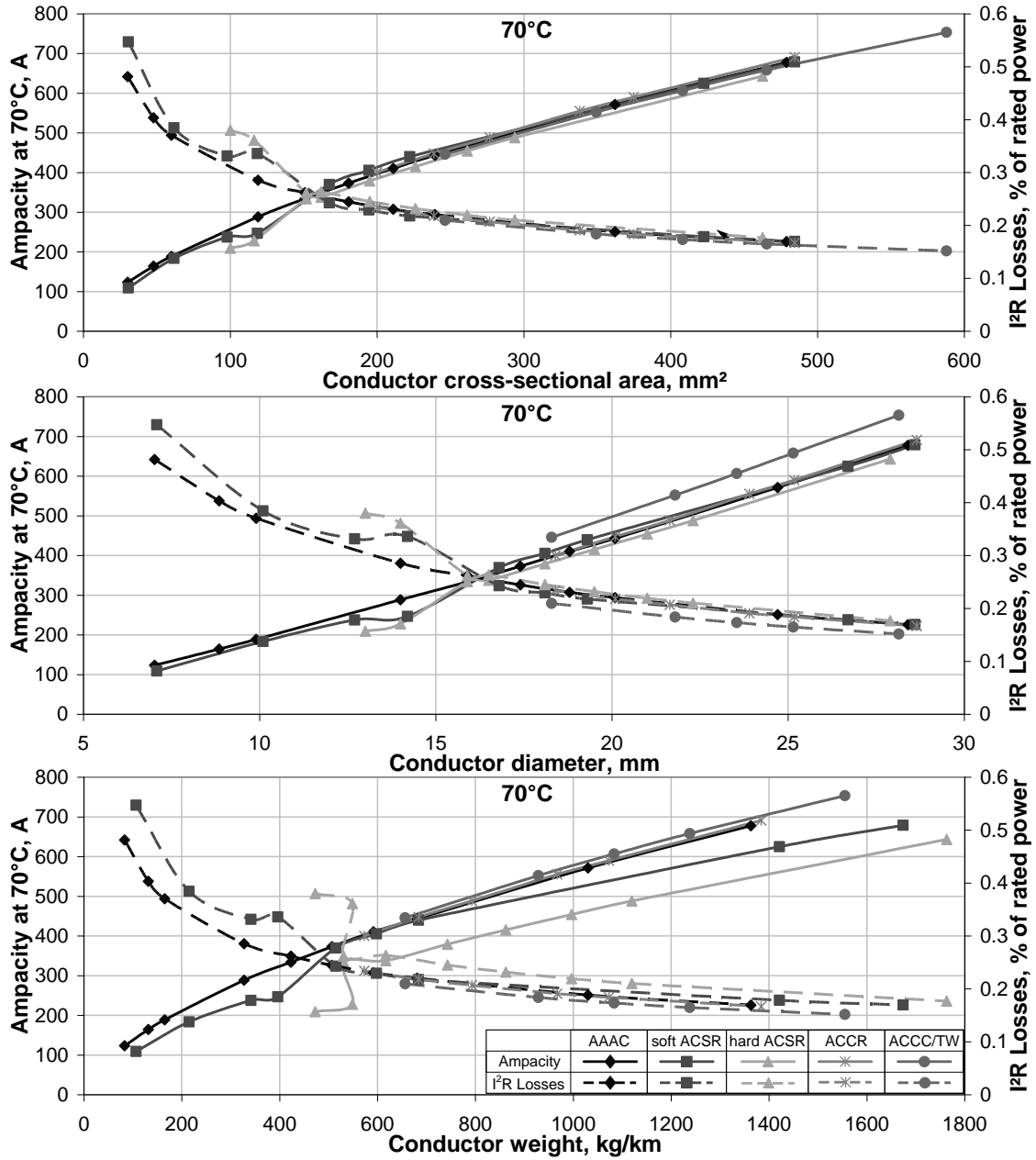


Figure 5

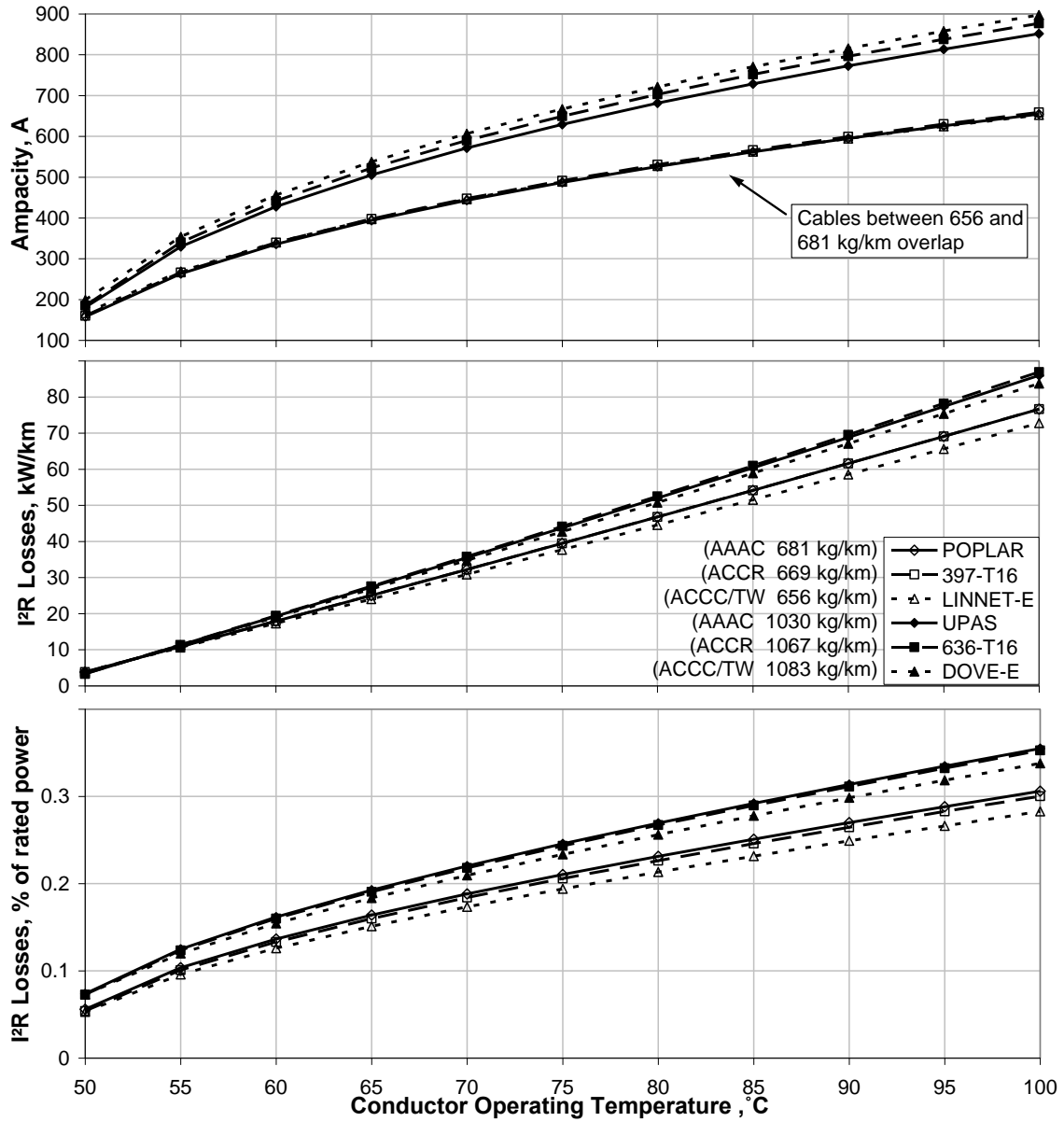


Figure 6

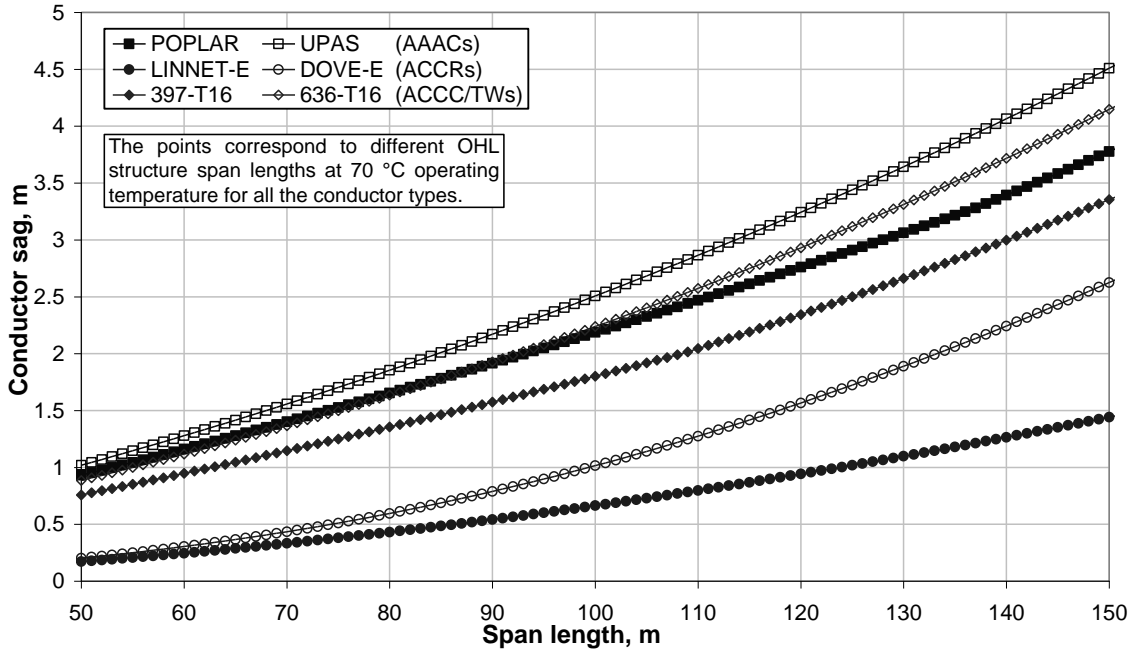


Figure 7

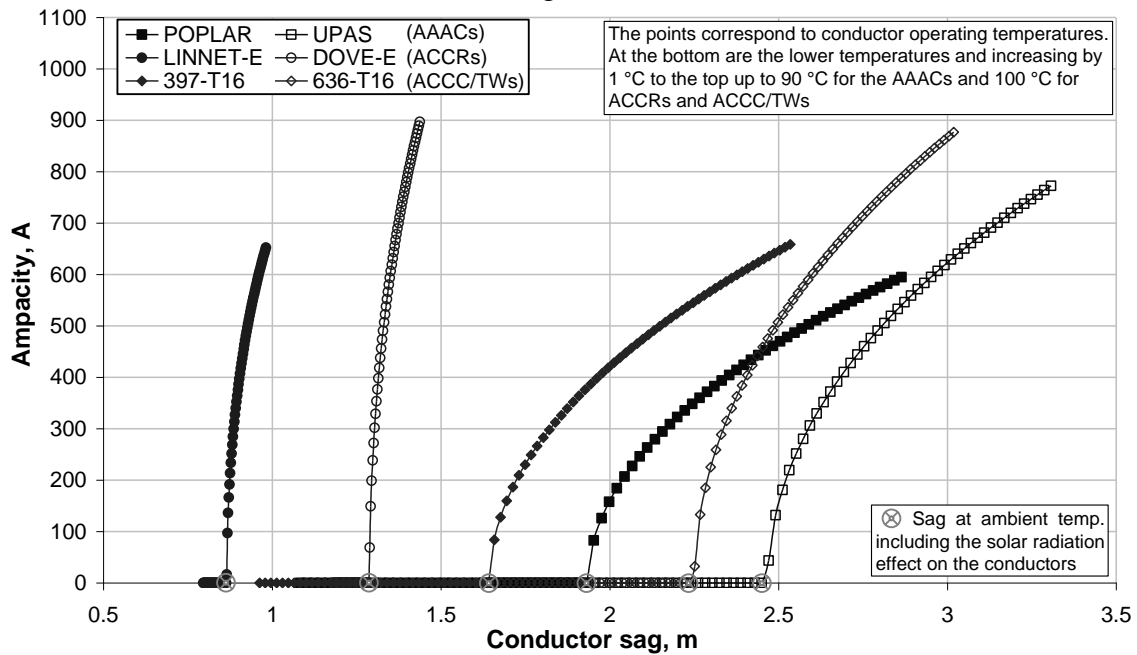


Figure 8